



## Cortical and subcortical response to the anticipation of reward in high and average/low risk-taking adolescents

Michael I. Demidenko<sup>a,\*</sup>, Edward D. Huntley<sup>b</sup>, Andrew Jahn<sup>c</sup>, Moriah E. Thomason<sup>d</sup>, Christopher S. Monk<sup>a,b</sup>, Daniel P. Keating<sup>a,b</sup>

<sup>a</sup> Department of Psychology, University of Michigan, Ann Arbor, United States

<sup>b</sup> Survey Research Center, Institute for Social Research, University of Michigan, Ann Arbor, United States

<sup>c</sup> The Functional MRI Laboratory, University of Michigan, Ann Arbor, United States

<sup>d</sup> Department of Child and Adolescent Psychiatry, New York University Langone, New York, United States

### ARTICLE INFO

#### Keywords:

Adolescent Health Risk Behaviors  
Maturational Imbalance  
Dual Systems  
Triadic  
Reward anticipation  
Adolescence

### ABSTRACT

Since the first neurodevelopmental models that sought to explain the influx of risky behaviors during adolescence were proposed, there have been a number of revisions, variations and criticisms. Despite providing a strong multi-disciplinary heuristic to explain the development of risk behavior, extant models have not yet reliably isolated neural systems that underlie risk behaviors in adolescence. To address this gap, we screened 2017 adolescents from an ongoing longitudinal study that assessed 15-health risk behaviors, targeting 104 adolescents (Age Range: 17-to-21.4), characterized as high-or-average/low risk-taking. Participants completed the Monetary Incentive Delay (MID) fMRI task, examining reward anticipation to “big win” versus “neutral”. We examined neural response variation associated with both baseline and longitudinal (multi-wave) risk classifications. Analyses included examination of *a priori* regions of interest (ROIs); and exploratory non-parametric, whole-brain analyses. Hypothesis-driven ROI analysis revealed no significant differences between high- and average/low-risk profiles using either baseline or multi-wave classification. Results of whole-brain analyses differed according to whether risk assessment was based on baseline or multi-wave data. Despite significant mean-level task activation, these results do not generalize prior neural substrates implicated in reward anticipation and adolescent risk-taking. Further, these data indicate that whole-brain differences may depend on how risk-behavior profiles are defined.

### 1. Introduction

Recognition has grown that adolescence is one of the highest health risk periods in human development, characterized as having the highest rates of preventable mortality and morbidity (Kann et al., 2018). This brings to the forefront the need to understand biological change and developmental variation underlying adolescence. In particular, knowledge about adolescent neurodevelopment has the potential to inform both policy-making and interventions for those at highest risk (Dahl et al., 2018). An overwhelming 70 % of adolescent deaths in the United States are related to preventable causes, with a similar proportion for morbidity, from behaviors such as suicide, homicide, risky driving, risky sex and substance use (Casey et al., 2008; Kann et al., 2018). Although it has been recognized that risky behaviors contribute to the increased rates of morbidity and mortality in adolescence, many programs that

have been developed to reduce those risky behaviors have been minimally effective (Ferdinand et al., 2015; Hale et al., 2014; Steinberg, 2008).

In order to characterize change in development, several efforts have contributed to neurodevelopmental models that attempt to explain the seeming incongruity of increased risky behaviors and improved reasoning skills during adolescence (Ernst et al., 2006; Shulman et al., 2016). This multi-disciplinary work has led to several neurodevelopmental models that have been influential in characterizing the developmental stage, with public policy implications (Shulman et al., 2016; Steinberg and Icenogle, 2019). However, the studies have received criticism due to the inconsistencies in findings and lack of convergence across key components of the models (Crone and Dahl, 2012; Meisel et al., 2019; Pfeifer and Allen, 2012; Sherman et al., 2018). Previous researchers proposed that these neurodevelopmental models

\* Corresponding author at: Department of Psychology, University of Michigan, 530 Church St. 2036, Ann Arbor, MI, 48109, United States.

E-mail address: [demidenm@umich.edu](mailto:demidenm@umich.edu) (M.I. Demidenko).

<https://doi.org/10.1016/j.dcn.2020.100798>

Received 13 January 2020; Received in revised form 5 May 2020; Accepted 15 May 2020

Available online 21 May 2020

1878-9293/© 2020 The Authors.

Published by Elsevier Ltd.

This is an open access article under the CC BY-NC-ND license

(<http://creativecommons.org/licenses/by-nc-nd/4.0/>).

may characterize a subset of youth that may be of highest risk (Bjork and Pardini, 2015), and a recent meta-analysis recommended taking a categorical approach by comparing qualitatively different “high risk-takers” to more normative risk profiles (Sherman et al., 2018, p. 37). This raises the question of whether recent modeling and sampling techniques of neurodevelopment models accurately characterize real world risk profiles?

Current theories of neurodevelopment in adolescence have focused on the socioemotional and cognitive control systems (Casey et al., 2008; Ernst et al., 2006; Luna and Wright, 2016; Steinberg, 2008). Socioemotional systems encompass reward sensitivity, such as sensation- and novelty-seeking. A common thread across theories is that changes in reward sensitivity encourage the adolescent to experiment with rewarding stimuli, such as social, sexual, substance and other risk behaviors. Sensation seeking is thought to be associated with basal dopamine (DA) levels that drive incentive motivation, which in turn enhances the engagement in a salient behavior (Ernst and Luciana, 2015; Ernst and Spear, 2009). Recent evidence suggests that sensation seeking (or reward sensitivity) peaks in late adolescence (around age 19; Steinberg et al., 2018). Meanwhile, the maturation of cognitive control systems relates to the progressive proliferation of white matter (WM) and grey matter (GM; (Mills et al., 2016; Tamnes et al., 2017), facilitating the specialization of cognitive processes and improvement in goal-oriented behaviors (Luna et al., 2010; Marek et al., 2015). A number of such dual process models (Shulman et al., 2016) are described in more detail below.

Despite broad similarities across current neurodevelopmental models in the process and function of socioemotional and cognitive systems, there are several key differences. The *Triadic model* (Ernst et al., 2006) focuses on the balance between approach, avoidant and regulatory systems. The approach system has positive valence, focused on rewarding stimuli, that drives an organism to engage in novel behaviors. Meanwhile, the avoidance system has negative valence, focused on harm, that is involved in operant and conditioned behavior to help notify the organism of whether a stimulus should (or should not) be approached. The third component is the regulatory, or cognitive control system, which is critical in monitoring and adaptation, functioning as a conductor to facilitate behaviors by balancing information across multiple systems (Ernst et al., 2006; Richards et al., 2013). The key systems in the Triadic model rely on different brain regions, specifically the approach system recruits both orbital frontal cortex (OFC) and ventral striatum (VS); the avoidance system primarily involves the amygdala (central nucleus for operant behavior and lateral/basolateral for conditioning stimuli) and insula; and the regulatory system involves the ventrolateral PFC (vlPFC), dorsolateral prefrontal cortex (dlPFC) and anterior cingulate cortex (ACC; Richards et al., 2013). All of these regions function in combination to exchange information and perform the goal-oriented behaviors.

As opposed to the balance across multiple systems in the Triadic model, *Maturational Imbalance* (Casey et al., 2008), *Dual Systems* (Steinberg, 2008) and *Driven Dual Systems* (Luna and Wright, 2016) models emphasize that the dominating or primary function of the cognitive control systems is to suppress inappropriate (or salient) thoughts and actions associated with the socioemotional system in favor of goal-oriented behaviors, reducing the effect of reward sensitivity. The *Maturational Imbalance* (Casey et al., 2008) model emphasizes that the inability to behave in a goal-oriented manner reflects immature development of the cognitive control system, supported by the vlPFC, which reduces the influence of reward sensitivity, supported by the Nucleus Accumbens (NAcc). In contrast, the *Dual Systems Model* (Steinberg, 2008) contends that decisions are a clash between cognitive control (mPFC/OFC/dlPFC) and social-emotional (Amygdala and VS) regions. The post-pubertal maturation of reward regions leads to increased reward seeking, especially in the context of peers, as a function of rising DA-rich receptors in the NAcc and decline in DA autoreceptors in the PFC, which function as a negative feedback loop, reducing the PFC's

ability to suppress inappropriate thoughts and actions. Similarly, the *Driven Dual Systems model* (Luna and Wright, 2016) contends that cognitive control is the key system in governing appropriate goal-oriented actions. In contrast to other models, this model suggests that cognitive control systems are largely developed by late childhood/early adolescence, and focuses instead on the hyperactivation of the reward regions (VS) due to the proliferation of DA receptors there that increases the appetitive/motivation systems and thus drive riskier behaviors.

Each of these neurodevelopmental models emphasizes the early sensitization of DA systems in reward regions following puberty, and the alteration of cognitive control and/or socioemotional systems as a function of improved cognitive capacity. They posit that these discrete systems interact as adolescents are exposed to salient stimuli. Notably, in all models, there is overlap in the brain regions that underlie reward, salience and cognitive control. Namely, socioemotional processing largely involves areas of the NAcc/VS and OFC; emotion processing is supported by the amygdala and mPFC; and cognitive control is attributed to regions of the dlPFC, ACC, OFC, and/or vlPFC.

Despite agreement about the brain regions involved in critical aspects of adolescent decision-making and behavior, there remains debate as to the variability in neural findings and associated behaviors attributed to these regions. fMRI has been an important tool in distinguishing neural differences associated with adolescence, yet a challenge in neurodevelopmental theories has been that while common regions are highlighted, the direction of effects in the literature is inconsistent. Some of the proposed regions in cognitive control systems have shown both activation and deactivation across age that have been difficult to reconcile (Crone and Dahl, 2012; Pfeifer and Allen, 2012). While some of these neural signatures of VS and PFC activation may be related to atypical development, they may not be representative of typically developing youth (Bjork and Pardini, 2015). As a result, the models imply predispositions in neurodevelopment in adolescence that bias them towards risky behaviors, resulting in post-hoc misinterpretation of differences as deficiencies rather than normative changes (Bjork and Pardini, 2015; Pfeifer and Allen, 2012). Moreover, the peaks in reward processing in the dual system models precede the peaks of unintentional and behavioral injury by several years, occurring between 18–23 (Bjork and Pardini, 2015; Kann et al., 2018; U.S. Centers for Disease Control, <https://www.cdc.gov/injury/wisqars/fatal.html>).

While the neurodevelopmental models have harnessed both animal and human research to test hypotheses about neural associations among psychological, neurobiological, and risk behavior development (Shulman et al., 2016), empirical efforts pertaining to convergent and ecological validity have been scant. One presumed association is in the neurobiological (reward sensitivity) and psychological (sensation seeking) pathways to risk taking behaviors (Shulman et al., 2016). A large proportion of studies investigating risk behaviors and neural change have relied on cognitive measures in laboratory settings as ‘scanner-compatible proxies for measuring real-world behaviors’ (Telzer et al., 2015, pp. 391) or ‘ecologically valid measure of real-life risk taking’ (Qu et al., 2015, pp. 11309). However, the use of proxy variables such as cognitive task performance to identify real-world risk behavior profiles as a dependent variable may be problematic owing to their questionable construct validity (Demidenko et al., 2019; Eisenberg et al., 2019). Specification and justification of these choices for measuring the dependent variable of risk behavior is thus paramount for efforts to accumulate and reproduce evidence on these questions.

Reviews that have examined neural predictors of risk behaviors in adolescents report substantial variability across studies that yield only mixed support for the neurodevelopmental models in the directions hypothesized above. More specifically, multiple reviews reported that comparison groups have had high variability in categorizing children, adolescents and adults (Crone and Dahl, 2012; Galván, 2010). Further, tasks have often utilized different analytic strategies, baseline conditions, and magnitudes (or probabilities) of reward. Sherman et al.

(2018) found in their review that risk taking indexed by different neural correlates is measured in different ways across studies, categorized, for example, by lab-based measures of risk in tasks (which may be largely ineffective, due to their weak associations with real-world risk behaviors), generalized sensation-seeking, or perceptions of risks. In addition, 70 % of the studies they reviewed were substantially underpowered ( $N < 50$ ) and oftentimes researchers solely used region of interest (ROI) approaches, focusing attention where findings were expected, overlooking alternative key regions posited by different neurodevelopmental models.

Although there have been longitudinal analyses that evaluate longitudinal changes in risk behaviors, the criteria used for age, targeted sampling, and measurements of risk may have contributed to some of the inconsistencies (Braams et al., 2015, 2016; Büchel et al., 2017; Cope et al., 2019). With respect to age, some studies used samples that included age ranges that were broad, 8–26 years (Braams et al., 2016), or outside of a window when risk behaviors peak (Bjork and Pardini, 2015), such as restricted to age 16 (Büchel et al., 2017). Other studies recruited in order to estimate effects of puberty (Braams et al., 2016; Peper et al., 2013) or populations in disadvantaged communities (Cope et al., 2019), making it difficult to discern neural correlates of risk behaviors in a normative adolescent population. This variability across studies has contributed to mixed findings of the neurodevelopmental models, whereby reward processing predicted substance use in Cope et al. (2019) but not in Braams et al. (2016), and only under the condition of high sensation seeking in Büchel et al. (2017). Thus, it remains unclear how risk profiles are associated with reward processing, recently reported to peak in late adolescence (age ~19; Steinberg et al., 2018), during corresponding developmental peaks in health risk behaviors (18–23 years) in a normative sample.

In the current study, we recruited a large and diverse population of typically developing high school adolescents (10th [15–16.5 years old] and 12th [17–19 years old] graders,  $N = 2017$  in the full sample) that provided self-reports on real-world risk behaviors in multiple categories. To address previous limitations of broad age ranges (Pfeifer and Allen, 2016), sampling and inefficient proxies of real-world risk, a targeted subsample ( $N = 104$ ) was recruited from the full sample, representing two distinct risk-taking profiles during late adolescence when risk behaviors often peak (Kann et al., 2018; U.S. Centers for Disease Control, <https://www.cdc.gov/injury/wisqars/fatal.html>). To characterize high versus average/low risk-taking adolescents that can appropriately contrast risk-taking profiles, the subsample of adolescents was classified into high (75th percentile and above) and average/low risk groups (20th – 60th percentile) based on a combined factor score of risk-taking self-reports, a Behavioral Misadventure Scale (BMS, based on a confirmatory factor analysis across all risk behavior categories). This subsample completed a neuroimaging protocol to evaluate differences in neural activity associated with the level of risk behavior derived from the Wave 1 BMS, utilizing both whole brain analyses and a list of key *a priori* brain regions (ROIs) from an empirical consensus based on the research literature (Galván, 2010; Sherman et al., 2018). In a subsequent comparison, high and average/low risk groups' neural activation profiles were assessed based on the longitudinal stability of their risk profiles over time, which has not been previously studied.

Given that the neurodevelopmental models propose an increased motivation (Shulman et al., 2016), or tonic levels of DA (Luciana and Collins, 2012), we examined neural differences towards the anticipation of a big reward. The Monetary Incentive Delay (MID) task used in the Adolescent Brain Cognitive Development (ABCD) study (Casey et al., 2018), similar to that used in the IMAGEN study (Cao et al., 2019), was administered during multi-band functional magnetic resonance imaging (fMRI) acquisition. This task has been shown to elicit robust activation of the NAcc, Insula, ACC and mPFC in the anticipation of reward, which have been reported to be sensitive to developmental and behavioral differences (Bjork et al., 2010; Cao et al., 2019; Knutson and Greer, 2008).

Using both whole brain and hypothesis-driven (ROI) approaches, this study was designed to test whether the neuroimaging results show the predicted differences between high versus average/low risk-taking adolescents. If risk-taking at or near its peak during adolescence is based in part on hyperactivation of incentive and reward systems, and still maturing prefrontal functions, we would predict that divergence to be reflected in the differences between high and average/low risk takers. Specifically, based on theoretical models and on previously reported neuroimaging studies, it was hypothesized: (1) that the MID task would demonstrate robust striatal activation; (2) compared to the average/low risk behavior group, the high risk group would exhibit increased VS, amygdala and/or OFC activation; and (3) the high risk group would exhibit decreased dlPFC activation.

## 2. Methods

### 2.1. Participants

Study characteristics are briefly summarized here with additional details regarding study design and methods described elsewhere (Demidenko et al., 2019). Participants in this neuroimaging study are a risk-taking classification-based subsample, invited to undergo MRI, of the Adolescent Health Risk Behavior (AHRB) study, which is designed to characterize behavioral, cognitive, psychosocial and neural correlates of adolescents' risk behavior trajectories. AHRB consists of a non-probability sample of 2017 ( $Age_{mean} = 16.8$ ,  $Age_{SD} = 1.1$ ; Female 56 %) 10th and 12th grade students recruited from nine public school districts across eight Southeastern Michigan counties. Study procedures were approved by the University of Michigan Institutional Review Board. From Phase I of the study, a subsample of 115 adolescents were recruited to participate in Phase 2, the neuroimaging phase of the study (average/low time after Wave 1:  $M = 30.9$  months,  $SD = 5.0$  months). Participants identified as belonging in high versus average/low risk behavior categories, based on a factor-analyzed Behavioral Misadventure Scale (BMS) that incorporated all risk behavior categories, were invited to participate in the neuroimaging phase. Of the 115 adolescents that participated, 108 completed the magnetic resonance imaging (MRI) portion of the visit. Seven participants ( $N = 6$ , average/low risk;  $N = 1$ , high risk) were ineligible or unable to participate in the MRI due to not meeting MRI safety eligibility/compatibility (e.g. claustrophobia ( $N = 3$ ) or no formally documented medical clearance to rule out potential metal in body ( $N = 4$ )). Of the 108 participants that completed the MRI, four participants were excluded from the analyses due to artifacts in the images that were not recoverable ( $N = 2$ , average/low risk;  $N = 1$ , high risk), and another due to ceasing to respond during the task ( $N = 1$ , average/low risk). The final fMRI subsample ( $N = 104$ ;  $Age_{Mean} = 18.9$ ,  $Age_{SD} = 1.3$ ; Female 57 %), of which  $N = 41$  were high-risk and  $N = 63$  average/low risk, was included in the subsequent analyses and did not differ from the full sample in age, gender, or time from the original survey.

### 2.2. Risk group classification: behavioral misadventure

A questionnaire assessed participants' self-reported engagement in 15 risk behaviors in the last 12-months. Risk behaviors included: using 1) cigarettes, 2) e-cigarettes, 3) alcohol, 4) marijuana, 5) amphetamines, 6) narcotics, 7) sedatives or 8) street drugs (including cocaine, heroin, ecstasy, and LSD); 9) distracted driving (e.g., texting while driving); 10) drowsy driving; 11) driving while under the influence of alcohol; 12) riding with an alcohol-impaired driver; 13) having unprotected sex; 14) physical fighting; and 15) other risks resulting in serious injury to oneself (e.g., riding a bicycle without a helmet). To summarize overall engagement in risk behavior and to give adequate weighting for low frequency but high health impact risk behaviors that could be used in identifying health risk profiles, the sample was randomized into two halves to conduct a principal component analysis (PCA) with the first

half and a confirmatory factor analysis (CFA) with the remaining half. Results were comparable and demonstrated satisfactory fit (Demidenko et al., 2019). A behavioral misadventure factor score (BMS), on which all of the risk behaviors loaded significantly, was saved for the entire sample and used in subsequent analyses (Cronbach  $\alpha = .78$ ). Based on this latent factor score, a high risk group was classified based on an 75th percentile cutoff, and an average/low risk group based on falling within the 20th to 60th percentile from the full Wave 1 sample ( $N = 2017$ ). This produced distinct groups that were non-overlapping (Figure S1). Our BMS variable had a strong association with a factor derived score of substance use (self-reported 12-month marijuana, alcohol, e-cigarettes, cigarettes, and illicit drug use; RMSEA: .08; CFI: .97; TLI: .95; SRMR: .03),  $r = .94$ , and the number of past 12-month self-reported health risk behaviors,  $r = .89$  during Wave 1.

## 2.3. fMRI task

To evaluate the neural activation of reward processing, the MID task reward (Knutson et al., 2000) was used to model the neural signatures of the anticipation of monetary reward (Cao et al., 2019; Bjork et al., 2010). The MID is a well-established task for assessing reward processing and is currently being employed across 21-sites in the national Adolescent Brain Cognitive Development (ABCD) study to measure the development of adolescent reward processing (Casey et al., 2018). Identical to the task described in Casey et al. (2018), the task in this study consists of three phases: anticipation, probe and outcome (that is, feedback). Each trial starts with a cue type (Win \$0.20, Win \$5, Lose \$5, Lose \$0.50, or No Money At Stake). Each cue lasts for 2000 ms and is followed by a jittered fixation cross (1500–4000 ms). Following the jittered fixation cross, the target probe cue (187–500 ms) appears that requires participants to respond in order to win or not lose money. If participants are too fast (or too slow), that trial is marked as incorrect. Following the probe phase, the outcome (or feedback) phase (2000 ms minus the target duration) indicates the outcome of that trial (for example, 'You Win \$5!', 'You Keep \$0.20', 'You Lose \$5' or 'No Money At Stake!'). There are twelve trial orders of the task, consisting of 50 contiguous trials and 10 trial types per run (5:42 min long). Participants complete two runs of the MID task during the scan (Total: 100 contiguous trials and 20 trials of each of five trial types). The task is individualized with an initial mean response time (MRT) that is used from the practice run performed outside of the scanner minutes before the scan. Using the mean reaction time (RT) plus two standard deviations on correct trials, the MID task individualizes the difficulty to reach around 60 % accuracy rate by adjusting the difficulty (that is, probe duration). See Figure S2 in Supplementary Materials for a schematic of the task.

Prior to the scan, participants were informed of all cue-related outcomes and completed a practice trial of the MID task. Participants were explicitly told that their performance on the task during the scan (for example, \$5 Win Cue is associated with an opportunity to win \$5 and a \$5 Lose cue was associated with an opportunity to not lose \$5) would be associated with the compensation they can get for their cumulative earnings during the MID (Maximum \$30). Stimuli were presented via the IFIS system (MRI Devices, Inc., Milwaukee, WI), an integrated stimulus display and experimental control package, also capable of recording button presses. Lenses were available with the IFIS system to correct subject vision, as needed.

## 2.4. fMRI data acquisition

Data were acquired using a GE Discovery MR750 3.0 T scanner with a standard adult-sized coil (Milwaukee, WI). A full-brain high-resolution T1 SPGR PROMO scan was acquired that is used in preprocessing (TR = 7000 ms, TE = 2900 ms, flip angle =  $8^\circ$ , FOV = 25.6 cm, slice thickness = 1 mm, 208 sagittal slices; matrix =  $256 \times 256$ ). Before the MID task, a fieldmap was acquired using spin-echo EPI (TR = 7400 ms, TE = 80 ms, FOV = 21.6 cm,  $90 \times 90$  matrix) with opposite phase encoding polarity

(A→P, P→A). Two functional T2\*-weighted BOLD MID runs were acquired in the axial plane using a multiband EPI sequence (MB factor = 6) of 60 contiguous axial 2.4 mm slices (TR = 800 ms, TE = 30 ms, flip angle =  $52^\circ$ , FOV = 21.6 cm,  $90 \times 90$  matrix, volumes = 407).

## 2.5. fMRI data analyses

fMRI data were reconstructed and realigned using SPM12, physiological noise was removed using RETROICOR (Glover et al., 2000), and a fieldmap correction was applied in SPM12 to each T2\* run to recover inhomogeneity of signal in the B0 field. Preprocessing steps were completed using FSL (FMRIB's Software Library, [www.fmrib.ox.ac.uk/fsl](http://www.fmrib.ox.ac.uk/fsl)) FEAT (FMRIB Expert Analysis Tool) Version 6.00. Our preprocessing steps included: registration to high resolution structural and standard space MNI 152 image using FLIRT (Jenkinson and Smith, 2001; Jenkinson, Bannister, Brady, & Smith, 2002), motion correction using MCFLIRT (Jenkinson et al., 2002), non-brain removal using BET (Smith, 2002), spatial smoothing using a Gaussian kernel of FWHM 5 mm, grand-mean intensity normalisation of the entire 4D dataset by a single multiplicative factor and high pass temporal filtering (Gaussian-weighted least-squares straight line fitting, with sigma = 50.0 s).

First-level analyses were performed by using FEAT. Time-series statistical analysis was carried out using FILM with local autocorrelation correction (Woolrich et al., 2001). Similar to other studies (Cao et al., 2019; Hagler et al., 2019; Lamm et al., 2014), both Anticipation and Feedback events were modeled (15 explanatory variables), in addition to six motion parameters [translation (XYZ) and rotation (pitch, roll, yaw)] as well as their derivatives for a total of 12 motion regressors. Anticipation events included: Big Win, (\$5.00) Small Win (\$0.20), Neutral (No money at stake), Small Lose (\$0.20) and Big Lose (\$5.00) condition cues. Feedback included both hit and miss events for: Big Win, Small Win, Neutral, Small Lose, Big Lose. To control for the temporal effect of motion of the BOLD signal, we used the command *fsl\_motion\_outliers* to generate an additional confound list censoring frame displacement (FD) volumes that exceeded  $FD > .9$ . To average/low across the two runs, a second-level model was defined for each participant using fixed effect analysis in FEAT.

## 2.6. Whole brain

Group-level analyses were performed using non-parametric permutation tests to create null non-parametric distributions and control type 1 error rates (Eklund et al., 2016), with cluster correction performed using Threshold-Free Cluster Enhancement (TFCE) in order to accurately differentiate both focal and broad level activation that may be lost using standard parametric models (Smith and Nichols, 2009; Winkler et al., 2014). As described in Pfeifer et al. (2019), nonparametric models reduce assumptions about spatial distributions of noise within fMRI and reduce false positive rates. A design matrix was used differentiating group (High versus Average/low risk), with a covariate of age that was demeaned and entered into the model. To perform the analysis, FSL's *randomise* command (5000 permutations) was used with *zstat* files produced from Feat Second Level's for reward anticipation, contrast Big Win > Neutral. A cluster-level threshold of FWE-corrected  $p < .05$  was used to identify significant values in the statistical maps for a mask (Supplementary Figure S3).

## 2.7. Regions of interest

*A priori* regions of interest (ROI) from Neurosynth ([www.neurosynth.org](http://www.neurosynth.org)) were used to evaluate differences of mean signal intensity for reward anticipation in high versus average/low risk groups. These regions were selected based on overlap in original descriptions of the dual systems models and from 18 studies (totaling 70 coordinates, with overlap; see Supplementary Table S1 and Figure S3a) described in two reviews of adolescent neurodevelopment and risk behavior (reviewed in



Galván, 2010; Sherman et al., 2018). Region labels (such as Nucleus Accumbens) from the review were used as the search terms in Neurosynth. Due to multiple peaks in the vmPFC region defined on Neurosynth, the NIFTI file was downloaded and thresholded in fsleyes in conjunction with coordinates from the 20 study meta-analysis that referred to the vmPFC. A central (ventral) peak from the Neurosynth ROI (see Figure S3b) was selected that overlapped visually with the coordinates from the ROI meta-analysis that was consistent with function in secondary rewards (Haber and Behrens, 2014). A list of Neurosynth MNI coordinates (Supplementary Table S2), were converted into voxel space. Based on previous task-based and resting fMRI procedures for ROI analyses, the central voxel coordinates for ROI's were used with *fsmaths* to create 10 mm spheres. For each ROI, the voxels from each contrast mask (using z-statistics produced by Feat Second Level) were averaged to create a mean signal intensity value that was extracted using *fsleants* and used in analyses in R version 3.6.1 (R Core Team, 2019). To control the type I error rate and consider relationships among ROI's that may differentiate risk and age profiles, a Multivariate analysis of variance (MANOVA) was performed. Subsequently, to examine the association between risk profile and mean signal intensity of each ROI, fourteen multiple regression models are performed, controlling for age. To control for multiple comparisons (14 multiple regression models), rather than using a highly conservative Bonferroni correction, a less conservative False Discovery Rate (FDR) was used, and adjusted p-values are reported where significant differences arise (Benjamini and Yekutieli, 2001; Noble, 2009). The FDR rate was calculated by including an array of p-values from the models of interest into the `p.adjust()` function in R ("BH" method), which returns an array of adjusted values. fMRI Scripts and files used in these ROI and permutation analyses (with associated output files) are available on github (<https://github.com/demidenko/AHRB/tree/master/RewardRisk>).

## 2.8. Post-hoc analyses

To evaluate the effects of stable, multi-wave, risk profile, a combination of waves administering self-report measures of risky behaviors were used to define 'stable high' (that is, 75th percentile or higher on two waves of survey response) and 'stable average/low' (20th-60th percentile on two waves) risk profiles. These profiles were used to re-examine the ROI and whole brain analyses to determine whether there are significant differences between the persistently high versus average/low risk behavior profiles used to predict neural activation. This method may evoke differing neural properties that may capture robust individual differences in problematic behaviors as opposed to a single self-reporting of risk engagement.

## 3. Results

### 3.1. Descriptive and behavioral

There were no significant group differences between overall performance (accuracy and response times) in the high and average/low risk groups ( $p > .05$ ) during MID trials, nor for big win or neutral trials (Table 1; Figure S5). Notably, response times were only collected by E-Prime for accurate trials, thus we report only the variation with regard to response times with respect to hit and not miss trials (Table S4; Figure S6). Moreover, there were no significant differences in time before wave 1 and scan 1 (Figure S7), sex, or parental education between groups ( $p > .05$ ).

Conversely, High risk ( $N = 41$ ) and average/low risk ( $N = 63$ ) groups varied with respect to age. Specifically, those in the high risk group were significantly older ( $p < .01$ ,  $d = .52$ ;  $M = 19.3$ ,  $SD = 1.4$ ) than those in the average/low risk group ( $M = 18.6$ ,  $SD = 1.3$ ; see Table 1). Due to the significant age-related difference found in sensitivity to reward processing in previous studies (Bjork et al., 2010; Dhingra et al., 2019), age was covaried out for in the subsequent analyses. Age significantly

**Table 1**

Demographic characteristics and behavioral performance of full sample completing the Monetary Incentive Delay Task by Risk Profile.

	Average/low $n = 63$	High $n = 41$	Total $n = 104$	Effect Size
Sex, Female $n$ (%)	37 (57.1)	22 (53.7)	59 (56.7)	$\Phi = .02$
Race, $n$ (%)				
Black, non-Hispanic	12 (19.0)	3 (7.3)	15 (14.4)	
White, non-Hispanic	40 (63.5)	34 (82.9)	74 (71.2)	
Other	5 (8.0)	1 (2.4)	6 (5.7)	
Hispanic/Latinx	6 (9.5)	3 (7.3)	9 (8.7)	
	$M$ ( $SD$ )	$M$ ( $SD$ )	$M$ ( $SD$ )	
Age	18.6 (1.3)	19.3 (1.4)	18.9 (1.3)	$d = .52^{**}$
Parental Education	4.4 (1.1)	4.1 (1.2)	4.3 (1.2)	$d = .26$
BMS	-0.28 (0.1)	0.83 (0.8)	0.16 (0.6)	$d = 1.95^{***}$
Overall Acc. %	57.4 (3.2)	56.2 (3.1)	56.9 (3.2)	$d = .38$
Win Big	63.7 (9.2)	61.2 (9.1)	62.7 (9.2)	$d = .27$
Win Small	56.8 (9.5)	59.3 (9.7)	57.8 (9.6)	$d = .26$
Neutral	49.8 (14.2)	44.5 (14.5)	47.7 (14.5)	$d = .37$
Lose Small	56.3 (9.5)	56.5 (7.7)	56.4 (8.8)	$d = .02$
Lose Big	60.2 (10.5)	59.4 (10.4)	59.9 (10.4)	$d = .08$

BMS = Behavioral Misadventure Score; WASI IQ = Wechsler Abbreviated Scale of Intelligence; Parental Education: 1 = grade school or less, 2 = Some High School, 3 = Completed High School, 4 = some college, 5 = completed college, 6 = graduate or professional school. Acc = Accuracy;  $d$  = Cohen's  $d$  (Small = .2; Medium = .5, large = .8).

$p < .05^*$ ,  $p < .01^{**}$ ,  $p < .001^{***}$ .

related with risk group ( $r = .30$ ) and the continuous BMS variable ( $r = .39$ ).

### 3.2. Region of interest (ROI) analyses

First, to examine the association reward anticipation and adolescent risk behaviors, we used hypothesis-driven *a priori* ROI's to examine recent theoretical models. To analyze the variance among the 14 ROI's, the MANOVA revealed no significant activation difference between risk profiles (average/low versus high), Wilk's lambda = .83  $F(14, 87) = 1.26$ ,  $p = .25$ , nor an interactive effect of risk group (high versus average/low) and age, Wilk's lambda = .93  $F(14, 87) = 0.93$ ,  $p = .53$ . This indicated that there were no adjusted-mean differences in reward anticipation activation among the fourteen ROI's that are associated with age or self-reported risk. In the multiple regression models examining the association between risk profile (high versus average/low risk) and activation to the anticipation of big reward versus neutral trials in 14 ROI's, controlling for age, there were no significant associations when correcting for multiple comparisons (Supplementary Table S3 for corrected and uncorrected values).

### 3.3. Whole brain analyses

Consistent with prior work using the MID task, our task evoked robust activation of the reward regions during reward anticipation, as hypothesized (Figure S8). To examine whether Wave 1 average/low risk ( $N = 63$ ) and Wave 1 high risk ( $N = 41$ ) groups differed in neural activation during reward anticipation, we conducted a nonparametric whole brain analysis (adjusted for age). Contrary to the hypothesized neurodevelopmental models, however, and reflecting inconsistencies in recent literature, there were no significant group differences in activation in regions specified in the neurodevelopmental models (e.g, aforementioned *a priori* ROI's). Moreover, the high-risk group ( $N = 41$ ) did not exhibit greater activation in any voxels/clusters as compared to the average/low risk group ( $N = 63$ ). However, consistent with recent evidence (Sherman et al., 2018), in a direct contrast between groups, the average/low risk group exhibited several significant clusters in the whole brain analysis as compared to the high risk group that were outside of the regions specified in the neurodevelopmental models. Specifically, the average/low risk group had greater activation ( $p < .05$ ;

FWE-Corrected) in the dorsal striatal, precuneus, posterior parietal, primary visual, primary cortex, and cerebellar regions (See Table 2; Fig. 1).

### 3.4. Post-hoc analysis of adolescents with risk-group transition

For the stable, multi-wave, comparison of risk profiles, reward anticipation for stable high and stable average/low were compared. As expected, there was a significant difference in the number of adolescents moving to high versus moving to the average/low risk group ( $\chi^2(3) = 94.6, p < .001, \phi = .98$ ), whereby 23 adolescents (Mean Age = 18.6, SD = 1.1) moved from the average/low group to the high risk group, and five adolescents (Mean Age = 19.0, SD = 1.4) moved from the high risk group to the average/low risk group when using multi-wave information to compose a stable risk profile. These groups did not significantly on age, sex, or parental education ( $p > .05$ ). After excluding adolescents that transitioned to different risk profiles ( $N = 27$ ) and those that did not complete a questionnaire in a subsequent wave ( $N = 6$ ), this reduced the subsample to 70 adolescents, 37 stable average/low risk (M Age = 18.6, SD = 1.3) and 33 stable high risk (Mean Age = 19.4, SD = 1.3) adolescents. Analyses between the stable high and average/low-risk groups afforded an opportunity for a more stringent test of this individual difference contrast.

### 3.5. Post-hoc region of interest analyses

The post-hoc analyses evaluating ROI differences in stable high versus stable average/low risk takers demonstrated comparable results

**Table 2**

Whole Brain Analyses: significant differences in activation for Average/low versus High Risk-taking adolescents to anticipation of big reward versus neutral contrast.

Wave 1 Average/low (N = 63) > High (N = 41) Risk-taking				
Cluster Index <sup>a</sup>	Cluster peak x, y, z	# of Voxels	Cluster Label <sup>b</sup>	p <sup>*</sup>
14	-15, -3, 16	722	Left-Caudate	.03
13	22, -62, -16	208	Right Cerebellar	.03
12	16, -82, 4	129	Right Primary Visual	.04
11	-22, -72, 2	70	Left Primary Visual	.04
10	-17, 23, 12	44	<sup>†</sup> Left-Caudate Nucleus	.04
9	6, -74, 10	36	Right Primary Visual	.04
8	-10, -60, 50	36	Left Precuneus	.04
7	18, -36, 34	25	<sup>†</sup> Posterior Cingulate	.04
6	-16, -50, -8	22	Left-Secondary Visual	.04
5	34, -30, 28	19	<sup>†</sup> Left-Parahippocampal	< .05
4	4, -40, 42	17	Posterior Cingulate	< .05
3	-4, -32, 62	11	Primary Motor	< .05
2	-4, -72, -2	10	Left Visual	< .05
Longitudinally Stable Average/low (N = 37) > Stable High (N = 33) Risk-Taking				
Cluster Index <sup>a</sup>	Cluster peak x, y, z	# of Voxels	Cluster Label <sup>b</sup>	p <sup>*</sup>
4	30, 32, 34	181	Right Dorsolateral Prefrontal Cortex	.052
3	-8, -60, 48	17	Left Precuneus	.071
2	4, 20, 40	15	Paracingulate Gyrus	.074

<sup>a</sup> Cluster index identified using *fsl* command *cluster* that identified peak clusters in volume, index 1 not reported due to number of voxels = < 3, clusters plotted on MNI brain in Figs. 1 and 2.

<sup>b</sup> To identify region for cluster label, we used a combination of reverse inference on neurosynth.org/locations to identify top association with cluster activation and cross-referenced with *FSL Harvard-Oxford Cortical Structural Atlas*.

<sup>c</sup> Implies regional association, due to peak being in white matter.

<sup>\*</sup> Probability  $\alpha < .05$  used to threshold results of TFCE output from randomize.

<sup>#</sup> Lowered  $\alpha < .08$  used to threshold results of TFCE output from randomise (< .05, results null).

to the wave 1 risk profile. Specifically, the analysis of variance among the 14 ROI's, the MANOVA revealed no significant association between risk profile (average/low versus high), Wilk's lambda = .67  $F(14, 53) = 1.82, p = .06$ , and no interactive effect of group of risk (high versus avg/low) and age, Wilk's lambda = .85  $F(14, 53) = 0.64, p = .81$ . Similar to Wave 1 risk profiles, stability of profiles over time did not reveal a relationship among the fourteen ROI's. Moreover, the fourteen multiple regression models revealed comparable results to the wave 1 risk groups. In the multiple regression models, when corrected for multiple comparisons, there were no significant associations (Supplementary Table S3 for corrected and uncorrected values).

### 3.6. Post-hoc analyses whole brain analyses

The post-hoc analysis evaluating the whole brain activation to the anticipation of big reward versus neutral condition in stable high versus stable average/low risk takers demonstrated different results from that of Wave 1 sample defining risk profiles. Specifically, the nonparametric TFCE analysis revealed no-significant clusters that surpassed the  $\alpha < .05$ . At a lower threshold of  $\alpha < .08$ , in a direct contrast between groups, revealed clusters that were significant in the initial analysis (See Table 2; Fig. 2), specifically greater activation in Left Precuneus ( $p = .07$ ) in average/low as compared high risk takers. Likewise, at a lower threshold ( $p < .08$ ), average/low risk takers demonstrated greater activation in Right dlPFC ( $p = .05$ ), and Paracingulate Gyrus ( $p = .07$ ). These results suggest slight convergence, while also variability between single versus multiple assessment of risk profiles in whole brain activation that necessitates increased power. Notably, using the Euclidean distance between peak coordinates

$$\sqrt{(x_{whole\ brain} - x_{ROI})^2 + (y_{whole\ brain} - y_{ROI})^2 + (z_{whole\ brain} - z_{ROI})^2}$$

used by Hong et al. (2019, pp. 387), comparing the peak location of dlPFC in the whole brain results to that of the *a priori* dlPFC coordinate, there was a 64.5 mm distance between peaks, suggesting difference in the location of peak activation. Further, similar to the subsample ( $N = 70$ ) and full sample ( $N = 104$ ), activation in right dlPFC was present only at a lower threshold,  $p = .05$  and  $p = .06$ , respectively. Statistical maps of tests and presentations of ROI's from meta-analysis coordinate spheres are available on Neurovault (neurovault.org/collections/6282/)

### 3.7. Sensitivity analyses

To examine whether there was a continuous effect of BMS and/or from Wave 1 on brain activation during Big Win Reward versus Neutral anticipation phase in MID task, we created a nonparametric model (FSL *randomise*) to test the continuous variable of BMS, Age and brain. The continuous BMS model, covaried for age, demonstrated no significant associations ( $p > .05$ ) between BMS and brain. However, at a lower bound threshold ( $p < .08$ ), comparable clusters were found in the continuous BMS model (Table S5) and the dichotomous comparison of High versus Average/Low risk groups (Table 2). This reduced effect in the continuous model may be explained by the increased variance explained between BMS and age (15%) versus risk group and age (9%). Meanwhile, no significant effect of age (continuous) on brain was present, with or without the covariate of the BMS in the nonparametric model.

## 4. Discussion

### 4.1. Neural differences of risk and behavior

Over the last 15 years, several neurodevelopmental models have been proposed as a way to explain in part the rise in risky behaviors during mid-to-late adolescence. Despite a strong commitment to exploring the neural differences in cognitive control and reward

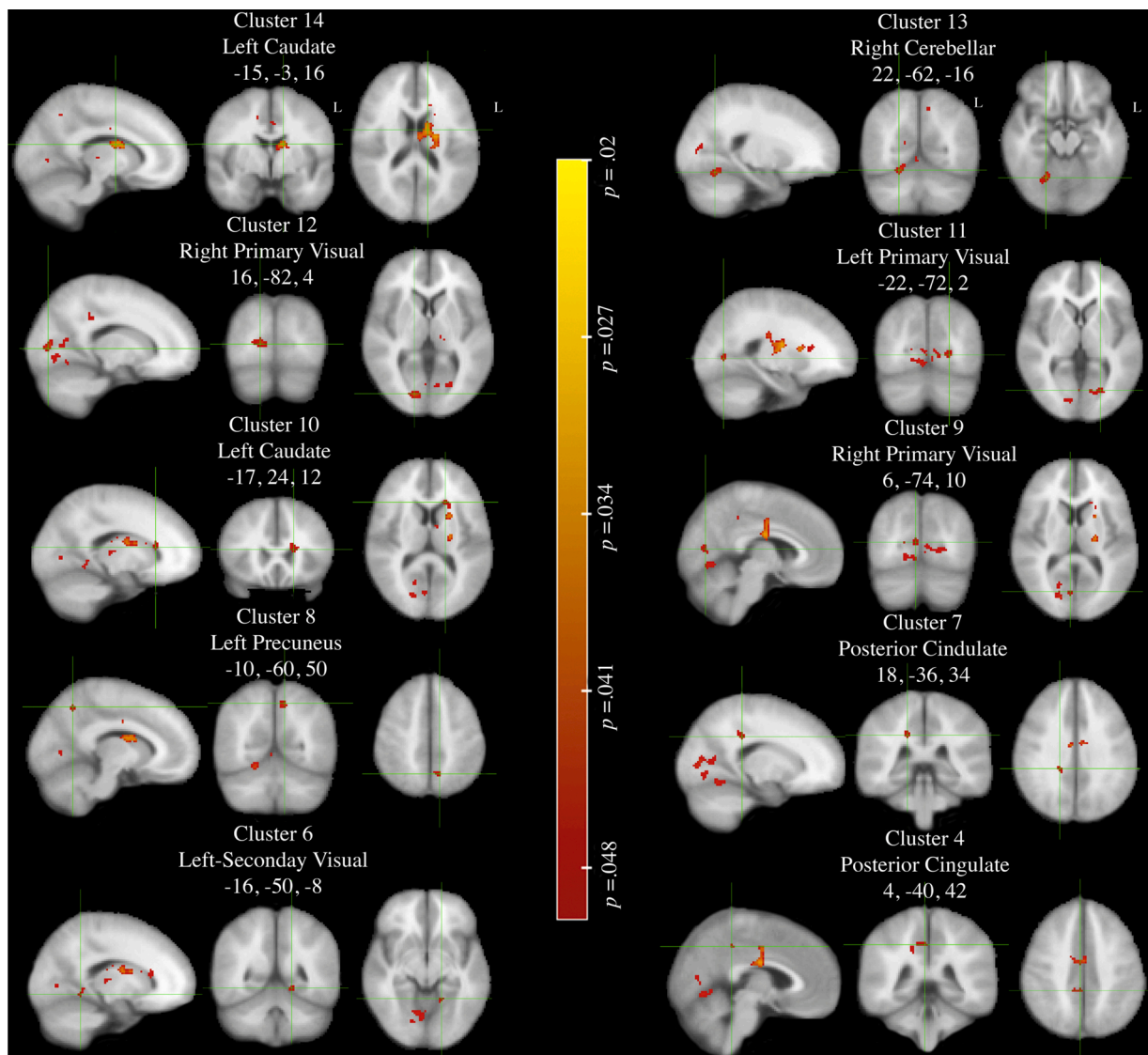


**Fig. 1.** Whole Brain Permutation Wave 1: Average/low > High Risk-Taking Profile during (FWE-corrected) anticipation of Big win versus Neutral contrast, thresholded  $p < .05$ .

Non-permutation test includes 5000 permutations, using FSL *randomise* with threshold-free cluster enhancement. Statistical maps thresholded at lower value .05 – clusters selected from Table 1.

processing across a broad age-range, inconsistencies in definitions of risk and parameter selection have led to mixed interpretations (Crone and Dahl, 2012). Furthermore, proxies of risk behaviors and *a priori* ROI analyses have contributed to heterogeneous results that have not replicated theoretical models (Sherman et al., 2018). To our knowledge, this study is the first to use several ecological measures to derive high and average/low risk behavior groups among adolescents, as well as longitudinally stable high versus average/low risk-taking profiles, to explore prospective neurodevelopmental differences using both *a priori* ROI and whole brain analyses. The variability in results and lack of generalizability or neurodevelopmental heuristics in prior studies may be related to sample sizes, independent variable and parameter selection, ROI identification, and an assumption of homogeneity in adolescents.

Using predefined ROI's based on neurodevelopmental models and prior literature, there was little evidence for increased recruitment of reward anticipatory neurocircuitry in high-risk versus average/low risk-taking adolescents. Although frequently researched regions, specifically the 'hot spots' of reward processing (Woo et al., 2017), such as the ventral striatum, did produce the predicted robust activation in statistical maps during the anticipation of a big monetary reward compared to

a neutral cue, this activation did not differentiate risk profiles among adolescents. In some ways, this latter finding supports the notion evoked by Sherman et al. (2018), whereby studies have not consistently found differences across risk-taking behaviors that are often cited by neurodevelopmental models.

To avoid constraining interpretations to *a priori* ROI's and behavioral properties of the task, a nonparametric analysis on the whole brain was conducted that revealed significant and non-significant results, varying across the defining criteria for high and average/low risk profiles. In the initial comparison that used self-report risk behavior measures from Wave 1, the comparison of high versus average/low risk takers revealed increased activation across a broad range of regions. These included the dorsal striatal, primary visual, primary motor, precuneus, posterior cingulate and cerebellar regions. However, when using more than one wave of risk behavior self-reports to identify stable high and average/low risk profiles, the activation differed from the Wave 1 whole brain analysis. Specifically, neither of the clusters of activation based on Wave 1 analysis were represented in the stable high and stable average/low risk analysis at a  $p < .05$  level. Taken together, the findings indicate differences in independent variable and parameter selection, whereby



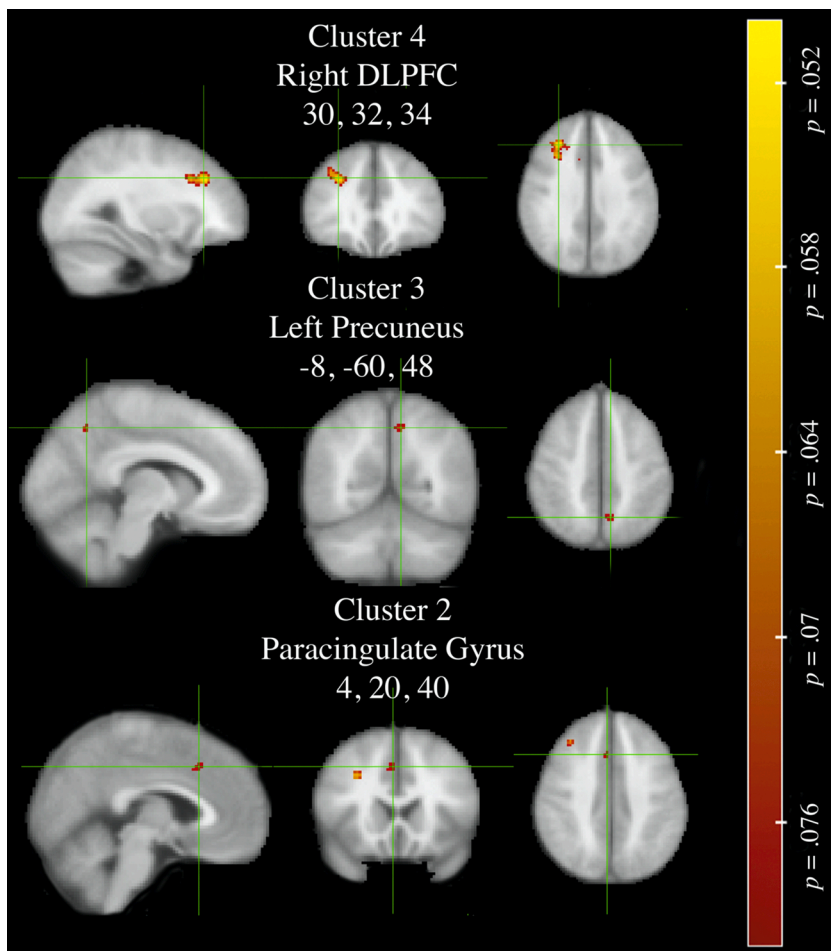


**Fig. 2.** Whole Brain Permutation Longitudinally Stable Average/low > High Risk-Taking during anticipation of Big win versus Neutral contrast, thresholded  $p < .08$  (FWE-corrected).

DLPFC = Dorsolateral prefrontal cortex. Non-permutation test includes 5000 permutations, using FSL *randomise* with threshold-free cluster enhancement. Statistical maps thresholded at lower value,  $p < .08$ , thresholding at .05 provided no significant differences – clusters selected from [Table 1](#).

power and the heterogeneity across subjects alters results.

Recent inconsistencies in findings can be attributed to multiple sources, such as sample sizes ([Button et al., 2013](#); [Cremers et al., 2017](#)), nonindependent analyses that may contribute to ‘voodoo’ correlations ([Vul et al., 2009](#)), or between-study task differences ([Sherman et al., 2018](#)). It is apparent from recent reviews that neuroimaging studies suffer from small samples, whereby the average/low sample size in adolescent risk behavior literature is <50 participants ([Galván, 2010](#); [Sherman et al., 2018](#)). [Cremers et al. \(2017\)](#) argued that small samples, such  $N = 30$ , are one source of misleading results. A review of early fMRI research demonstrated that often a strategy was to compute separate correlations of voxels/clusters with behavior that exceeded a threshold in a group level map, where these correlations with behavior on occasion even exceeded intraclass correlations of regions of interest ([Vul et al., 2009](#)). Some of these correlations are attributable to extremely small samples that systematically inflate correlation between neural activation and behavior ([Yarkoni et al., 2009](#)). Furthermore, differences in tasks and contrasts used in studies are often overlooked. In the 23 studies of adolescent risk taking reviewed by [Sherman et al. \(2018\)](#), it is evident that several different tasks are administered in the literature, such as the MID, Stoplight signal, Wheel of Fortune, Iowa Gambling, and Coin-flip task, which likely vary in the cognitive processes they engage ([Richards et al., 2013](#)). These between-study differences of tasks make it difficult to discern the generalizability of neural correlates with behavior. Animal models have demonstrated that learning what to and not to approach is variable, while some circuits are related to prediction error, others may be related to goal-oriented models ([Eshel and Steinberg, 2018](#)). For example, the MID, wheel of fortune or balloon analogue risk task may relate to distinct circuits that show an important role for

learning the action and event values through trial and error, whereas affective and peer paradigms may relate to efferent working models that make decisions regarding future events that may impact goal-directed choice. In the latter decision-based model, values are estimated with each action using inferences based on costs, benefits and some forms of neural signals ability to generalize to new situations ([Rangel and Hare, 2010](#); [Schultz, 2015](#)).

Distinctions in how decisions are made may be critical as there are heterogeneities in animal behaviors, whereby some rely on a trial-and-error and others on goal-directed choice ([Eshel and Steinberg, 2018](#)). With respect to neural properties, such intricacies of connections may impact the region of activation. Although the VS/NAcc dominate the core locations of risk/reward processing in the neurodevelopmental models, neural processing may depend on various aspects, some of which include: type of learning (or encoding paradigm); whether the processing relates to afferent or efferent systems; whether a reward is contingent on action and if a reward is primary or secondary ([Haber and Behrens, 2014](#); [Padoa-Schioppa and Conen, 2017](#); [Szczepanski and Knight, 2014](#)). These distinctions are critical in assessing whether results do (or do not) converge across studies and have a similar predictive utility.

Studies evaluating the central tenets of the neurodevelopmental models have largely interpreted the task activation of VS/NAcc to reflect incentive salience (or motivation to act) which may be associated with risky behaviors, however, incentive salience may also be related to attentional processes and so may be difficult to disentangle using abstract task contrasts. There is growing evidence that the VS (which includes the NAcc) is actively involved in effort and intrinsic motivation ([Schoupe et al., 2014](#)), which can be associated with value ([Inzlicht](#)



et al., 2018). Therefore, activity during task performance in some brain regions, such as the VS/NAcc and dorsal striatum, may reflect an interactive effect of reward and attention (Breckel et al., 2011; Krebs et al., 2012). Such that, reward and attention may arise from similar neural mechanisms (Westbrook and Braver, 2016), making it difficult to derive an accurate assessment of reward using abstract methods of subtraction in task-based fMRI (Poldrack and Yarkoni, 2016). To derive improved estimates of reward or risky decision-making in task-based fMRI, increasing attention should be given to the construct validity of tasks and their presumed estimates of cognitive processes, such as incentive salience (Demidenko et al., 2020).

Outside of the domain of neural estimates, there is substantial heterogeneity in the behavioral definition of risky behaviors. Research on normative samples often utilizes variables that may not be ecologically valid proxies of real-world risk behavior. While some use psychological characteristics such as sensation seeking (Demidenko et al., 2020), general measures of risky behaviors (Op de Macks et al., 2016; Saxbe et al., 2015), substance use (Bjork et al., 2011; Chung et al., 2015) or likelihood of engaging in future risk (Galvan et al., 2007), several studies associate neural activation as a function of risk as measures by the task, such as driving (Cascio et al., 2015), probability or gambling tasks (Eshel et al., 2007; Op de Macks et al., 2016; Qu et al., 2015; Telzer et al., 2015). These proxy-based measures of risky behavior may be inappropriate as laboratory tasks that may require larger samples to capture small effects (Sherman et al., 2018) and that have limited evidence for age-related differences (Defoe et al., 2015), and often serve as poor predictors of real-world risk behaviors in normative adolescent populations (Demidenko et al., 2019).

For neurodevelopmental models to be used as indicators of sensation seeking and risk behaviors, it is important to acknowledge that adolescent behavior is heterogeneous and that this behavior should be modeled as such (Bjork and Pardini, 2015; Sherman et al., 2018). With respect to the dynamic system of the brain, the assumption that individuals are homogenous is often violated (Beltz et al., 2016), and thus it is important to identify unique and similar patterns in the individuals that may be used systematically to more effectively explain behavioral change (Beltz & Gates, 2017). This alternative technique may be more appropriate in identifying networks, which were proposed in earlier reviews (Pfeifer and Allen, 2012), that may offer some stability of measurement within and between participants, as opposed to the mean-level task effects that often have poor test-retest reliability (Elliott et al., 2019). For example, although two substance users on paper may look similar, the neural activation may vary as a function of attention, motivation, or pleasure that are based on differential reward signals (Schultz, 2015), resulting in mean-activation during events of a task that will vary, but may reflect similar patterns in their neural dynamics that are missed in a ‘pooling’ of activation. Alternatively, since the location of activation in a particular region may vary between samples (or individuals), such as the dorsal anterior cingulate may vary between samples (Hong et al., 2019), response-patterns or heterarchical systems may be an alternative method to model differences in location, timing or interactions of neural activation (Haxby et al., 2011; Pessoa, 2017). Moving forward, a measure that accounts for the brain being a dynamic and plastic system may be more appropriate to speculate about the interaction of neural systems, how these systems change across tasks and time, and what the underlying neural signatures of risk taking may entail.

#### 4.2. Limitations

Although this study attempts to quantify risk behaviors in developing adolescents, the limitation of our analysis is that some of our parameters vary from previous studies. Prior work evaluating risk behaviors and neural activation incorporated cross-sectional and longitudinal analyses differing across parameters in task and definition of risk. For example, in cross-sectional samples, while Benningfield et al. (2014) examined the

association between discounting (as measured by Monetary Choice Questionnaire) and differences in activation to big, small and neutral rewards, Claus et al. (2018) examined the moderating effect of substance use on the association between brain activation and risk-taking tendencies on the Balloon Analogue Risk Task (BART). Further, in longitudinal analyses of adolescent risk behaviors, whereas Qu et al. (2015) explored the mediating effect of ventral striatal activation on the association between parent-child relationships and risk-taking on the BART, Braams, van Duijvenvoorde, Peper, & Crone (2015) examined associations between changes in nucleus accumbens response during a Two Choice task (heads or tails) and risk performance as captured by the BART and self-report measure of Behavior Inhibition System/Behavior Action System. Not surprisingly, due to variability in definition of risk and parameters, results varied from study to study. This degree of variability has also been reported for within-task contrasts, such as the MID (Demidenko et al., 2020).

Importantly, our study focused on individual differences among adolescents, and thus the results do not capture age-related change that is represented in the neurodevelopmental models. This study focused on variation across risk profiles, both cross-sectionally and longitudinally, to determine whether risk behavior variability among adolescents at or near the developmental peak of risk taking can be explained by neural activation that has been posited in previous models. Activation in adolescent risk profiles, in this analysis, cannot be attributed to either of the developmental models. Although age-related effects were not present here, the age-related trends may still be evident in the models, but the heuristics may not necessarily provide the evidence necessary to explain differences between adolescents who do and do not engage in risk behaviors, as was previously suggested (Spear, 2000).

#### 4.3. Conclusion

This is the first study to our knowledge to examine differences in neural activation across real-world risk profiles (from multiple waves) and a focal-age range when risk behaviors peak in adolescents. The results in this study demonstrate the previous hypothesized models did not explain the variation in risk profiles, and whole brain differences may depend on how risk profiles are defined. Moreover, common hot spots of reward related research, such as the ventral striatum, do not differentiate general risk profiles among adolescents, even though the task elicited a robust overall activation pattern that replicates prior research. This posits an important reassessment of how risk is captured and modeled in the developing adolescent brain, in order to improve predictive utility, interpretation for interventions, and generalizability and reproducibility of results.

#### Author's contribution

DK and MD conceptualized the study, MD conceived and conducted the statistical analysis, wrote the draft of the manuscript and AJ provided support with the analyses. DK, EH, designed and executed the survey and the neuroimaging protocol, with input from CM, and MT. DK, EH, CM, MT and AJ assisted MD with study conception and writing. All authors read and approved the manuscript.

#### Declaration of Competing Interest

The authors declare that they have no conflicts of interest.

#### Acknowledgments

This research was supported, in part, by a grant from the Eunice Kennedy Shriver National Institute of Child Health & Human Development (NICHD; R01HD075806, D.P. Keating, Principal Investigator). The effort was also supported by the NICHD Developmental Psychology Training Grant (5T32HD007109-34, V.C. McLoyd & C.S. Monk). The

authors thank Bennet Fauber, Krisanne Litinas, Christine Wagner, Peter Batra, Joshua Hatfield, Meredith House, Kyle Kwaiser, Kathleen LaDronka, the U-M Survey Research Operations staff and the U-M MRI Laboratory, for their support.

## Appendix A. Supplementary data

Supplementary material related to this article can be found, in the online version, at doi:<https://doi.org/10.1016/j.dcn.2020.100798>.

## References

- Beltz, A.M., Gates, K.M., 2017. Network mapping with GIMME. *Multivariate Behav. Res.* 52 (6), 789–804. <https://doi.org/10.1080/00273171.2017.1373014>.
- Beltz, A.M., Wright, A.G.C., Sprague, B.N., Molenaar, P.C.M., 2016. Bridging the nomothetic and idiographic approaches to the analysis of clinical data. *Assessment* 23 (4), 447–458. <https://doi.org/10.1177/1073191116648209>.
- Benjamini, Y., Yekutieli, D., 2001. The control of the false discovery rate in multiple testing under dependency. *Ann. Stat.* 29 (4), 1165–1188. <https://doi.org/10.1214/aos/1013699998>.
- Benningfield, M.M., Blackford, J.U., Ellsworth, M.E., Samanez-Larkin, G.R., Martin, P.R., Cowan, R.L., Zald, D.H., 2014. Caudate responses to reward anticipation associated with delay discounting behavior in healthy youth. *Dev. Cogn. Neurosci.* 7, 43–52. <https://doi.org/10.1016/j.dcn.2013.10.009>.
- Bjork, J.M., Pardini, D.A., 2015. Who are those “risk-taking adolescents”? Individual differences in developmental neuroimaging research. *Dev. Cogn. Neurosci.* 11, 56–64. <https://doi.org/10.1016/j.dcn.2014.07.008>.
- Bjork, J.M., Smith, A.R., Chen, G., Hommer, D.W., 2010. Adolescents, adults and rewards: comparing motivational neurocircuitry recruitment using fMRI. *PLoS One* 5 (7), e11440. <https://doi.org/10.1371/journal.pone.0011440>.
- Bjork, J.M., Smith, A.R., Chen, G., Hommer, D.W., 2011. Psychosocial problems and recruitment of incentive neurocircuitry: exploring individual differences in healthy adolescents. *Dev. Cogn. Neurosci.* 1 (4), 570–577. <https://doi.org/10.1016/j.dcn.2011.07.005>.
- Braams, B.R., van Duijvenvoorde, A.C.K., Peper, J.S., Crone, E.A., 2015. Longitudinal changes in adolescent risk-taking: a comprehensive study of neural responses to rewards, pubertal development, and risk-taking behavior. *J. Neurosci.* 35 (18), 7226–7238. <https://doi.org/10.1523/JNEUROSCI.4764-14.2015>.
- Braams, B.R., Peper, J.S., van der Heide, D., Peters, S., Crone, E.A., 2016. Nucleus accumbens response to rewards and testosterone levels are related to alcohol use in adolescents and young adults. *Dev. Cogn. Neurosci.* 17, 83–93. <https://doi.org/10.1016/j.dcn.2015.12.014>.
- Breckel, T.P.K., Giessing, C., Thiel, C.M., 2011. Impact of brain networks involved in vigilance on processing irrelevant visual motion. *NeuroImage* 55 (4), 1754–1762. <https://doi.org/10.1016/j.neuroimage.2011.01.025>.
- Büchel, C., Peters, J., Banaschewski, T., Bokke, A.L.W., Bromberg, U., Conrod, P.J., Flor, H., Papadopoulos, D., Garavan, H., Gowland, P., Heinz, A., Walter, H., Ittermann, B., Mann, K., Martinot, J.-L., Paillère-Martinot, M.-L., Nees, F., Paus, T., Pausova, Z., et al., 2017. Blunted ventral striatal responses to anticipated rewards foreshadow problematic drug use in novelty-seeking adolescents. *Nat. Commun.* 8 (1), 1–11. <https://doi.org/10.1038/ncomms14140>.
- Button, K.S., Ioannidis, J.P.A., Mokrysz, C., Nosek, B.A., Flint, J., Robinson, E.S.J., Munafò, M.R., 2013. Power failure: why small sample size undermines the reliability of neuroscience. *Nat. Rev. Neurosci.* 14 (5), 365–376. <https://doi.org/10.1038/nrn3475>.
- Cao, Z., Bennett, M., Orr, C., Icke, I., Banaschewski, T., Barker, G.J., Bokke, A.L.W., Bromberg, U., Büchel, C., Quinlan, E.B., Desrivieres, S., Flor, H., Frouin, V., Garavan, H., Gowland, P., Heinz, A., Ittermann, B., Martinot, J.-L., Nees, F., et al., 2019. Mapping adolescent reward anticipation, receipt, and prediction error during the monetary incentive delay task. *Hum. Brain Mapp.* 40 (1), 262–283. <https://doi.org/10.1002/hbm.24370>.
- Cascio, C.N., Carp, J., O'Donnell, M.B., Tinney, F.J., Bingham, C.R., Shope, J.T., Ouimet, M.C., Pradhan, A.K., Simons-Morton, B.G., Falk, E.B., 2015. Buffering social influence: neural correlates of response inhibition predict driving safety in the presence of a peer. *J. Cogn. Neurosci.* 27 (1), 83–95. [https://doi.org/10.1162/jocn\\_a.00693](https://doi.org/10.1162/jocn_a.00693).
- Casey, B.J., Getz, S., Galvan, A., 2008. The adolescent brain. *Dev. Rev.* 28 (1), 62–77. <https://doi.org/10.1016/j.dr.2007.08.003>.
- Casey, B.J., Cannonier, T., Conley, M.I., Cohen, A.O., Barch, D.M., Heitzeg, M.M., Soules, M.E., Teslovich, T., Dellarco, D.V., Garavan, H., Orr, C.A., Wager, T.D., Banich, M.T., Speer, N.K., Sutherland, M.T., Riedel, M.C., Dick, A.S., Bjork, J.M., Thomas, K.M., ABCD Imaging Acquisition Workgroup, ..., 2018. The adolescent brain cognitive development (ABCD) study: imaging acquisition across 21 sites. *Dev. Cogn. Neurosci.* 32, 43–54. <https://doi.org/10.1016/j.dcn.2018.03.001>.
- Chung, T., Paulsen, D.J., Geier, C.F., Luna, B., Clark, D.B., 2015. Regional brain activation supporting cognitive control in the context of reward is associated with treated adolescents' marijuana problem severity at follow-up: A preliminary study. *Dev. Cogn. Neurosci.* 16, 93–100. <https://doi.org/10.1016/j.dcn.2015.05.004>.
- Claus, E.D., Feldstein Ewing, S.W., Magnan, R.E., Montanaro, E., Hutchison, K.E., Bryan, A.D., 2018. Neural mechanisms of risky decision making in adolescents reporting frequent alcohol and/or marijuana use. *Brain Imaging Behav.* 12 (2), 564–576. <https://doi.org/10.1007/s11682-017-9723-x>.
- Cope, L.M., Martz, M.E., Hardee, J.E., Zucker, R.A., Heitzeg, M.M., 2019. Reward activation in childhood predicts adolescent substance use initiation in a high-risk sample. *Drug Alcohol Depend.* 194, 318–325. <https://doi.org/10.1016/j.drugalcdep.2018.11.003>.
- Creemers, H.R., Wager, T.D., Yarkoni, T., 2017. The relation between statistical power and inference in fMRI. *PLoS One* 12 (11), e0184923. <https://doi.org/10.1371/journal.pone.0184923>.
- Crone, E.A., Dahl, R.E., 2012. Understanding adolescence as a period of social-affective engagement and goal flexibility. *Nat. Rev. Neurosci.* 13 (9), 636–650. <https://doi.org/10.1038/nrn3313>.
- Dahl, R.E., Allen, N.B., Willbrecht, L., Suleiman, A.B., 2018. Importance of investing in adolescence from a developmental science perspective. *Nature* 554 (7693), 441–450. <https://doi.org/10.1038/nature25770>.
- Defoe, I.N., Dubas, J.S., Figner, B., van Aken, M.A.G., 2015. A meta-analysis on age differences in risky decision making: adolescents versus children and adults. *Psychol. Bull.* 141 (1), 48–84. <https://doi.org/10.1037/a0038088>.
- Demidenko, M.I., Huntley, E.D., Martz, M.E., Keating, D.P., 2019. Adolescent health risk behaviors: convergent, discriminant and predictive validity of self-report and cognitive measures. *J. Youth Adolesc.* 48 (9), 1765–1783. <https://doi.org/10.1007/s10964-019-01057-4>.
- Demidenko, M.I., Ganesan, K., Weigard, A.S., Jang, H., Jahn, A.A., Huntley, E., Keating, D.P., 2020. Interactions Between Methodological and Interindividual Variability: How Monetary Incentive Delay (MID) Task Contrast Maps Vary and Impact Associations With Behavior. <https://doi.org/10.31234/osf.io/9fasc>.
- Dhingra, I., Zhang, S., Zhornitsky, S., Le, T.M., Wang, W., Chao, H.H., Levy, I., Li, C.-S.R., 2019. The effects of age on reward magnitude processing in the monetary incentive delay task. *NeuroImage*. <https://doi.org/10.1016/j.neuroimage.2019.116368>, 116368.
- Eisenberg, I.W., Bissett, P.G., Zeynep Enkavi, A., Li, J., MacKinnon, D.P., Marsch, L.A., Poldrack, R.A., 2019. Uncovering the structure of self-regulation through data-driven ontology discovery. *Nat. Commun.* 10 (1), 1–13. <https://doi.org/10.1038/s41467-019-10301-1>.
- Eklund, A., Nichols, T.E., Knutsson, H., 2016. Cluster failure: why fMRI inferences for spatial extent have inflated false-positive rates. *Proc. Natl. Acad. Sci. U. S. A.* 113 (28), 7900–7905. <https://doi.org/10.1073/pnas.1602413113>.
- Elliott, M.L., Knodt, A.R., Ireland, D., Morris, M.L., Poulton, R., Ramrakha, S., Sison, M. L., Moffitt, T.E., Caspi, A., Hariri, A.R., 2019. Poor test-retest reliability of task-fMRI: new empirical evidence and a meta-analysis. *BioRxiv*. <https://doi.org/10.1101/681700>.
- Ernst, M., Luciana, M., 2015. Neuroimaging of the dopamine/reward system in adolescent drug use. *CNS Spectr.* 20 (4), 427–441. <https://doi.org/10.1017/S1092852915000395>.
- Ernst, M., Spear, L.P., 2009. Reward systems. *Handbook of Developmental Social Neuroscience*. The Guilford Press, pp. 324–341.
- Ernst, M., Pine, D.S., Hardin, M., 2006. Triadic model of the neurobiology of motivated behavior in adolescence. *Psychol. Med.* 36 (3), 299–312. <https://doi.org/10.1017/S0033291705005891>.
- Eshel, N., Steinberg, E.E., 2018. Learning what to approach. *PLoS Biol.* 16 (10), e3000043. <https://doi.org/10.1371/journal.pbio.3000043>.
- Eshel, N., Nelson, E.E., Blair, J., Pine, D.S., Ernst, M., 2007. Neural substrates of choice selection in adults and adolescents: development of the ventrolateral prefrontal and anterior cingulate cortices. *Neuropsychologia* 45 (6), 1270–1279. <https://doi.org/10.1016/j.neuropsychologia.2006.10.004>.
- Ferdinand, A.O., Menachemi, N., Blackburn, J.L., Sen, B., Nelson, L., Morrissey, M., 2015. The impact of texting bans on motor vehicle crash-related hospitalizations. *Am. J. Public Health* 105 (5), 859–865. <https://doi.org/10.2105/AJPH.2014.302537>.
- Galván, A., 2010. Adolescent development of the reward system. *Front. Hum. Neurosci.* 4. <https://doi.org/10.3389/fnhum.0006.2010>.
- Galvan, A., Hare, T., Voss, H., Glover, G., Casey, B.J., 2007. Risk-taking and the adolescent brain: who is at risk? *Dev. Sci.* 10 (2), F8–F14. <https://doi.org/10.1111/j.1467-7687.2006.00579.x>.
- Glover, G.H., Li, T.Q., Ress, D., 2000. Image-based method for retrospective correction of physiological motion effects in fMRI: RETROICOR. *Magn. Reson. Med.* 44 (1), 162–167. [https://doi.org/10.1002/1522-2594\(200007\)44:1<162::aid-mrm23>3.0.co;2-e](https://doi.org/10.1002/1522-2594(200007)44:1<162::aid-mrm23>3.0.co;2-e).
- Haber, S.N., Behrens, T.E.J., 2014. The neural network underlying incentive-based learning: implications for interpreting circuit disruptions in psychiatric disorders. *Neuron* 83 (5), 1019–1039. <https://doi.org/10.1016/j.neuron.2014.08.031>.
- Hagler, J.V., Hattton, S., Cornejo, M.D., Makowski, C., Fair, D.A., Dick, A.S., Sutherland, M.T., Casey, B.J., Barch, D.M., Harms, M.P., Watts, R., Bjork, J.M., Garavan, H.P., Hilmer, L., Pung, C.J., Sicut, C.S., Kuperman, J., Bartsch, H., Xue, F., et al., 2019. Image processing and analysis methods for the adolescent brain cognitive development study. *NeuroImage* 202, 116091. <https://doi.org/10.1016/j.neuroimage.2019.116091>.
- Hale, D.R., Fitzgerald-Yau, N., Viner, R.M., 2014. A systematic review of effective interventions for reducing multiple health risk behaviors in adolescence. *Am. J. Public Health* 104 (5), e19–e41. <https://doi.org/10.2105/AJPH.2014.301874>.
- Haxby, J.V., Guntupalli, J.S., Connolly, A.C., Halchenko, Y.O., Conroy, B.R., Gobbini, M. I., Hanke, M., Ramadge, P.J., 2011. A common, high-dimensional model of the representational space in human ventral temporal cortex. *Neuron* 72 (2), 404–416. <https://doi.org/10.1016/j.neuron.2011.08.026>.
- Hong, Y.-W., Yoo, Y., Han, J., Wager, T.D., Woo, C.-W., 2019. False-positive neuroimaging: undisclosed flexibility in testing spatial hypotheses allows presenting anything as a replicated finding. *NeuroImage* 195, 384–395. <https://doi.org/10.1016/j.neuroimage.2019.03.070>.

- Inzlicht, M., Shenhav, A., Olivola, C.Y., 2018. The effort paradox: effort is both costly and valued. *Trends Cogn. Sci.* 22 (4), 337–349. <https://doi.org/10.1016/j.tics.2018.01.007>.
- Jenkinson, M., Smith, S., 2001. A global optimisation method for robust affine registration of brain images. *Med. Image Anal.* 5 (2), 143–156.
- Jenkinson, M., Bannister, P., Brady, M., Smith, S., 2002. Improved optimization for the robust and accurate linear registration and motion correction of brain images. *NeuroImage* 17 (2), 825–841.
- Kann, L., McManus, T., Harris, W.A., Shanklin, S.L., Flint, K.H., Queen, B., Lowry, R., Chyen, D., Whittle, L., Thornton, J., Lim, C., Bradford, D., Yamakawa, Y., Leon, M., Brener, N., Ethier, K.A., 2018. Youth risk behavior surveillance—United States, 2017. *Morbidity Mortal. Week. Rep. Surveill. Summar.* (Washington, D.C.: 2002) 67 (8), 1–114. <https://doi.org/10.15585/mmwr.ss6708a1>.
- Knutson, B., Greer, S., 2008. Anticipatory affect: neural correlates and consequences for choice. *Philos. Trans. R. Soc. B: Biol. Sci.* 363 (1511), 3771–3786. <https://doi.org/10.1098/rstb.2008.0155>.
- Knutson, B., Westdorp, A., Kaiser, E., Hommer, D., 2000. fMRI visualization of brain activity during a monetary incentive delay task. *NeuroImage* 12 (1), 20–27. <https://doi.org/10.1006/nimg.2000.0593>.
- Krebs, R.M., Boehler, C.N., Roberts, K.C., Song, A.W., Woldorff, M.G., 2012. The involvement of the dopaminergic midbrain and cortico-striatal-thalamic circuits in the integration of reward prospect and attentional task demands. *Cereb. Cortex* 22 (3), 607–615. <https://doi.org/10.1093/cercor/bhr134>.
- Lamm, C., Benson, B.E., Guyer, A.E., Perez-Edgar, K., Fox, N.A., Pine, D.S., Ernst, M., 2014. Longitudinal study of striatal activation to reward and loss anticipation from mid-adolescence into late adolescence/early adulthood. *Brain Cogn.* 89, 51–60. <https://doi.org/10.1016/j.bandc.2013.12.003>.
- Luciana, M., Collins, P.F., 2012. Incentive Motivation, Cognitive Control, and the Adolescent Brain: Is It Time for a Paradigm Shift? *Child Dev. Perspect.* 6 (4), 392–399. <https://doi.org/10.1111/j.1750-8606.2012.00252.x>.
- Luna, B., Wright, C., 2016. Adolescent brain development: implications for the juvenile criminal justice system. *APA Handbook of Psychology and Juvenile Justice*. American Psychological Association, pp. 91–116. <https://doi.org/10.1037/14643-005>.
- Luna, B., Padmanabhan, A., O’Hearn, K., 2010. What has fMRI told us about the development of cognitive control through adolescence? *Brain Cogn.* 72 (1), 101–113. <https://doi.org/10.1016/j.bandc.2009.08.005>.
- Marek, S., Hwang, K., Foran, W., Hallquist, M.N., Luna, B., 2015. The contribution of network organization and integration to the development of cognitive control. *PLoS Biol.* 13 (12), e1002328. <https://doi.org/10.1371/journal.pbio.1002328>.
- Meisel, S.N., Fosco, W.D., Hawk, L.W., Colder, C.R., 2019. Mind the gap: a review and recommendations for statistically evaluating dual systems models of adolescent risk behavior. *Dev. Cogn. Neurosci.* 39, 100681. <https://doi.org/10.1016/j.dcn.2019.100681>.
- Mills, K.L., Goddings, A.-L., Herting, M.M., Meuwese, R., Blakemore, S.-J., Crone, E.A., Dahl, R.E., Güroglu, B., Raznahan, A., Sowell, E.R., Tamnes, C.K., 2016. Structural brain development between childhood and adulthood: convergence across four longitudinal samples. *NeuroImage* 141, 273–281. <https://doi.org/10.1016/j.neuroimage.2016.07.044>.
- Noble, W.S., 2009. How does multiple testing correction work? *Nat. Biotechnol.* 27 (12), 1135–1137. <https://doi.org/10.1038/nbt1209-1135>.
- Op de Macks, Z.A., Bunge, S.A., Bell, O.N., Wilbrecht, L., Kriegsfeld, L.J., Kayser, A.S., Dahl, R.E., 2016. Risky decision-making in adolescent girls: the role of pubertal hormones and reward circuitry. *Psychoneuroendocrinology* 74, 77–91. <https://doi.org/10.1016/j.psychneuro.2016.08.013>.
- Padoa-Schioppa, C., Conen, K.E., 2017. Orbitofrontal cortex: a neural circuit for economic decisions. *Neuron* 96 (4), 736–754. <https://doi.org/10.1016/j.neuron.2017.09.031>.
- Peper, J.S., Koolschijn, P.C.M.P., Crone, E.A., 2013. Development of risk taking: contributions from adolescent testosterone and the orbito-frontal cortex. *J. Cogn. Neurosci.* 25 (12), 2141–2150. <https://doi.org/10.1162/jocn.a.00445>.
- Pessoa, L., 2017. A network model of the emotional brain. *Trends Cogn. Sci.* 21 (5), 357–371. <https://doi.org/10.1016/j.tics.2017.03.002>.
- Pfeifer, J.H., Allen, N.B., 2012. Arrested development? Reconsidering dual-systems models of brain function in adolescence and disorders. *Trends Cogn. Sci.* 16 (6), 322–329. <https://doi.org/10.1016/j.tics.2012.04.011>.
- Pfeifer, J.H., Allen, N.B., 2016. The audacity of specificity: moving adolescent developmental neuroscience towards more powerful scientific paradigms and translatable models. *Dev. Cogn. Neurosci.* 17, 131–137. <https://doi.org/10.1016/j.dcn.2015.12.012>.
- Pfeifer, J., Flournoy, J., Cheng, T., Cosme, D., Flannery, J., Vijayakumar, N., Chavez, S., Jankowski, K., Byrne, M.L., Macks, Z.O., 2019. Improving Practices and Inferences in DCN. <https://osf.io/y9h8z/>.
- Poldrack, R.A., Yarkoni, T., 2016. From brain maps to cognitive ontologies: informatics and the search for mental structure. *Annu. Rev. Psychol.* 67 (1), 587–612. <https://doi.org/10.1146/annurev-psych-122414-033729>.
- Qu, Y., Fuligni, A.J., Galvan, A., Telzer, E.H., 2015. Buffering effect of positive parent-child relationships on adolescent risk taking: a longitudinal neuroimaging investigation. *Dev. Cogn. Neurosci.* 15, 26–34. <https://doi.org/10.1016/j.dcn.2015.08.005>.
- R Core Team, 2019. R: A Language and Environment for Statistical Computing. R Foundation for Statistical Computing. <https://www.R-project.org/>.
- Rangel, A., Hare, T., 2010. Neural computations associated with goal-directed choice. *Curr. Opin. Neurobiol.* 20 (2), 262–270. <https://doi.org/10.1016/j.conb.2010.03.001>.
- Richards, J.M., Plate, R.C., Ernst, M., 2013. A systematic review of fMRI reward paradigms used in studies of adolescents vs. adults: the impact of task design and implications for understanding neurodevelopment. *Neurosci. Biobehav. Rev.* 37 (5), 976–991. <https://doi.org/10.1016/j.neubiorev.2013.03.004>.
- Saxbe, D., Piero, L.D., Immordino-Yang, M.H., Kaplan, J., Margolin, G., 2015. Neural correlates of adolescents’ viewing of parents’ and peers’ emotions: associations with risk-taking behavior and risky peer affiliations. *Soc. Neurosci.* 10 (6), 592–604. <https://doi.org/10.1080/17470919.2015.1022216>.
- Schouppe, N., Demanet, J., Boehler, C.N., Ridderinkhof, K.R., Notebaert, W., 2014. The role of the striatum in effort-based decision-making in the absence of reward. *J. Neurosci.* 34 (6), 2148–2154. <https://doi.org/10.1523/JNEUROSCI.1214-13.2014>.
- Schultz, W., 2015. Neuronal reward and decision signals: from theories to data. *Physiol. Rev.* 95 (3), 853–951. <https://doi.org/10.1152/physrev.00023.2014>.
- Sherman, L., Steinberg, L., Chein, J., 2018. Connecting brain responsivity and real-world risk taking: strengths and limitations of current methodological approaches. *Dev. Cogn. Neurosci.* 33, 27–41. <https://doi.org/10.1016/j.dcn.2017.05.007>.
- Shulman, E.P., Smith, A.R., Silva, K., Icenogle, G., Duell, N., Chein, J., Steinberg, L., 2016. The dual systems model: review, reappraisal, and reaffirmation. *Dev. Cogn. Neurosci.* 17, 103–117. <https://doi.org/10.1016/j.dcn.2015.12.010>.
- Smith, S.M., 2002. Fast robust automated brain extraction. *Hum. Brain Mapp.* 17 (3), 143–155. <https://doi.org/10.1002/hbm.10062>.
- Smith, S.M., Nichols, T.E., 2009. Threshold-free cluster enhancement: addressing problems of smoothing, threshold dependence and localisation in cluster inference. *NeuroImage* 44 (1), 83–98. <https://doi.org/10.1016/j.neuroimage.2008.03.061>.
- Spear, L.P., 2000. The adolescent brain and age-related behavioral manifestations. *Neurosci. Biobehav. Rev.* 24 (4), 417–463.
- Steinberg, L., 2008. A social neuroscience perspective on adolescent risk-taking. *Dev. Rev.* 28 (1), 78–106. <https://doi.org/10.1016/j.dr.2007.08.002>.
- Steinberg, L., Icenogle, G., 2019. Using developmental science to distinguish adolescents and adults under the law. *Ann. Rev. Dev. Psychol.* 1 (1), 21–40. <https://doi.org/10.1146/annurev-devpsych-121318-085105>.
- Steinberg, L., Icenogle, G., Shulman, E.P., Breiner, K., Chein, J., Bacchini, D., Chang, L., Chaudhary, N., Giunta, L.D., Dodge, K.A., Fanti, K.A., Lansford, J.E., Malone, P.S., Oburu, P., Pastorelli, C., Skinner, A.T., Sorbring, E., Tapanya, S., Tirado, L.M.U., et al., 2018. Around the world, adolescence is a time of heightened sensation seeking and immature self-regulation. *Dev. Sci.* 21 (2). <https://doi.org/10.1111/desc.12532>.
- Szczepanski, S.M., Knight, R.T., 2014. Insights into human behavior from lesions to the prefrontal cortex. *Neuron* 83 (5), 1002–1018. <https://doi.org/10.1016/j.neuron.2014.08.011>.
- Tamnes, C.K., Herting, M.M., Goddings, A.-L., Meuwese, R., Blakemore, S.-J., Dahl, R.E., Güroglu, B., Raznahan, A., Sowell, E.R., Crone, E.A., Mills, K.L., 2017. Development of the cerebral cortex across adolescence: a multisample study of inter-related longitudinal changes in cortical volume, surface area, and thickness. *J. Neurosci.* 37 (12), 3402–3412. <https://doi.org/10.1523/JNEUROSCI.3302-16.2017>.
- Telzer, E.H., Fuligni, A.J., Lieberman, M.D., Miermicki, M.E., Galván, A., 2015. The quality of adolescents’ peer relationships modulates neural sensitivity to risk taking. *Soc. Cogn. Affect. Neurosci.* 10 (3), 389–398. <https://doi.org/10.1093/scan/nsu064>.
- Vul, E., Harris, C., Winkielman, P., Pashler, H., 2009. Puzzlingly high correlations in fMRI studies of emotion, personality, and social cognition. *Persp. Psychol. Sci.* 4 (3), 274–290. <https://doi.org/10.1111/j.1745-6924.2009.01125.x>.
- Westbrook, A., Braver, T.S., 2016. Dopamine does double duty in motivating cognitive effort. *Neuron* 89 (4), 695–710. <https://doi.org/10.1016/j.neuron.2015.12.029>.
- Winkler, A.M., Ridgway, G.R., Webster, M.A., Smith, S.M., Nichols, T.E., 2014. Permutation inference for the general linear model. *NeuroImage* 92, 381–397. <https://doi.org/10.1016/j.neuroimage.2014.01.060>.
- Woo, C.-W., Chang, L.J., Lindquist, M.A., Wager, T.D., 2017. Building better biomarkers: brain models in translational neuroimaging. *Nat. Neurosci.* 20 (3), 365–377. <https://doi.org/10.1038/nn.4478>.
- Woolrich, M.W., Ripley, B.D., Brady, M., Smith, S.M., 2001. Temporal autocorrelation in univariate linear modeling of fMRI data. *NeuroImage* 14 (6), 1370–1386. <https://doi.org/10.1006/nimg.2001.0931>.
- Yarkoni, T., 2009. Big correlations in little studies: inflated fMRI correlations reflect low statistical power—commentary on vul et al. (2009). *Persp. Psychol. Sci.* 4 (3), 294–298. <https://doi.org/10.1111/j.1745-6924.2009.01127.x>.